Cell Transplantation, Vol. 23, pp. 59–72, 2014
Printed in the USA.

0963-6897/14 $90.00 + .00
DOI: http://dx.doi.org/10.3727/096368912X659880
E-ISSN 1555-3892
www.cognizantcommunication.com

Pancreatic Islet Basement Membrane Loss and Remodeling After Mouse Islet Isolation and Transplantation: Impact for Allograft Rejection

H. F. Irving-Rodgers,* F. J. Choong,† K. Hummitzsch,‡
C. R. Parish,† R. J. Rodgers,‡ and C. J. Simeonovic†

*Institute of Health and Biomedical Innovation, Queensland University of Technology, Kelvin Grove, Queensland, Australia
†Department of Immunology, The John Curtin School of Medical Research, The Australian National University, Canberra, Australian Capital Territory, Australia
‡Research Centre for Reproductive Health, Discipline of Obstetrics and Gynaecology, Robinson Institute, The University of Adelaide, Adelaide, South Australia, Australia

The isolation of islets by collagenase digestion can cause damage and impact the efficiency of islet engraftment and function. In this study, we assessed the basement membranes (BMs) of mouse pancreatic islets as a molecular biomarker for islet integrity, damage after isolation, and islet repair in vitro as well as in the absence or presence of an immune response after transplantation. Immunofluorescence staining of BM matrix proteins and the endothelial cell marker platelet endothelial cell adhesion molecule-1 (PECAM-1) was performed on pancreatic islets in situ, isolated islets, islets cultured for 4 days, and islet grafts at 3–10 days posttransplantation. Flow cytometry was used to investigate the expression of BM matrix proteins in isolated islet β-cells. The islet BM, consisting of collagen type IV and components of Engelbreth–Holm–Swarm (EHS) tumor laminin 111, laminin α2, nidogen-2, and perlecan in pancreatic islets in situ, was completely lost during islet isolation. It was not reestablished during culture for 4 days. Peri- and intraislet BM restoration was identified after islet isotransplantation and coincided with the migration pattern of PECAM-1$^+$ vascular endothelial cells (VECs). After islet allotransplantation, the restoration of VEC-derived peri-islet BMs was initiated but did not lead to the formation of the intraislet vasculature. Instead, an abnormally enlarged peri-islet vasculature developed, coinciding with islet allograft rejection. The islet BM is a sensitive biomarker of islet damage resulting from enzymatic isolation and of islet repair after transplantation. After transplantation, remodeling of both peri- and intraislet BMs restores β-cell–matrix attachment, a recognized requirement for β-cell survival, for isografts but not for allografts. Preventing isolation-induced islet BM damage would be expected to preserve the intrinsic barrier function of islet BMs, thereby influencing both the effector mechanisms required for allograft rejection and the antirejection strategies needed for allograft survival.

Key words: Islet; Basement membrane (BM); Vascular endothelial cells (VECs); Transplantation; Isograft; Allograft; Rejection

INTRODUCTION

The vast improvement in islet transplant survival and function using the steroid-free Edmonton protocol of immunosuppression or variations of it (10,14,15,43,44) has led to a resurgence in the clinical transplantation of islets for the treatment of insulin-dependent or type 1 diabetes. Nevertheless, because of the heavy immunosuppression required, the criteria for patient selection have largely been restricted to the persistence of brittle diabetes and ineffective insulin therapy. Excessive numbers of islets (up to 10,000 islet equivalents per kilogram body weight) have been used to alleviate the need for insulin treatment of transplantation patients, and usually this has dictated the necessity for multiple islet donors (15) and stringent donor selection (15,43). Even then, long-term normoglycemia (>5 years) is not consistently achieved (10,15,43). Factors contributing to these problems include islet damage and loss of viability due to bystander effects of the enzymatic digestion of the donor pancreas, the impact of hypoxia on islet survival before islet revascularization after transplantation, long-term toxic effects of immunosuppression, and autoimmune damage and/or allograft rejection. Experimental studies have revealed that the isolation process results in loss of islet innervation (36), disruption of islet microvasculature (18), and apoptosis of β-cells due to significant loss of intracellular stores of the glycosaminoglycan heparan sulfate (57) and to detachment from the extracellular matrix (ECM) (50,51,55). It is generally

Received June 7, 2012; final acceptance November 20, 2012. Online prepub date: December 4, 2012.
Address correspondence to Dr. Charmaine J. Simeonovic, Department of Immunology, The John Curtin School of Medical Research, The Australian National University, Canberra, ACT 2601, Australia. E-mail: Charmaine.Simeonovic@anu.edu.au

accepted that such changes to islet architecture negatively impact islet survival and function early after transplantation and necessitate the transfer of excessive numbers of islets to compensate for this loss.

Efforts to minimize damage of human islets by overdigestion of the pancreas are currently focused on the critical assessment of cocktails of collagenolytic and proteolytic enzymes (1,2,10,15,16,30,43). Indeed, previous studies reported that mantled islets isolated with a rim of acinar tissue attached to the islet periphery (40) functioned significantly better than highly purified islets (51). This improvement was attributed to the retention of islet-associated ECM or islet basement membrane (BM), and thus the prevention of matrix detachment-induced apoptosis (anoikis) (12,50). In contrast, analyses of individual matrix proteins have revealed that purified islets lack peripheral staining for laminin (37,54,55) and collagen (37,54,55), supporting the notion that islets lose their BM during the isolation process (11,50). Such studies, however, have been incomplete and largely disadvantaged by the unavailability of appropriate reagents. Recently, we confirmed that mouse islets in situ are surrounded by a continuous BM comprising all of the conventional matrix protein components: laminin, collagen type IV, nidogen, and the heparan sulfate proteoglycan (HSPG) perlecan (17). This was a significant finding because the HSPG constituent, in particular, provides BMs with a barrier function that prevents cell invasion (33) and hence represents an intrinsic defense mechanism for islets in situ (17,57).

In addition to providing a barrier function, BMs also provide structural support for adjacent cells and play a role in separating tissues into different compartments (23,35). In particular, the islet BM provides a source of specialized ECM to which islet cells located at the periphery can attach via integrin–matrix protein interactions (23,37,54). Pancreatic islets in situ are highly vascularized, and cross-sections show that each intraislet capillary is surrounded by 8–10 islet β-cells (4,31), suggesting that the vascular endothelial BM within islets may also function as an ECM for attachment of islet cells located more distantly from the islet boundary and within the islet core (28). The previous report of a "double BM" surrounding capillaries within human islets in situ also supports this notion (53). In any case, it is reasonable to predict that an islet isolation process that disrupts both the islet BM and intraislet vascular endothelial BM is likely to lead to extensive islet cell apoptosis or anoikis due to matrix detachment.

In this study, we set out (i) to examine a panel of islet BM matrix proteins (laminins, collagen type IV, nidogen, and perlecan) in isolated mouse islets and compared this profile with the status before their isolation, after culture, and after transplantation; (ii) to ascertain the potential for BM repair in islets in vitro and after transplantation; (iii) to identify a mechanism of BM recovery; and (iv) to investigate the likely impact of BM remodeling on islet engraftment and β-cell–matrix attachment in islet isografts and during allograft rejection. Our studies reveal that islet isolation induces dramatic loss of the islet BM. We observed complete repair of the islet BM only after isotransplantation, a process that is most likely due to vascular endothelial cells (VECs). Recovery of islet BMs was often incomplete after allotransplantation. Such partial repair of the barrier function of islet BMs would render the islets highly vulnerable to mononuclear cell (MNC) invasion during rejection. These findings highlight the islet BM as a critical biomarker for islet integrity in vitro and in vivo.

MATERIALS AND METHODS

Animals

CBA (H-2^k) and C57BL/6 (H-2^b) male mice, 6–13 weeks old, were obtained from the Australian National University Bioscience Facility, Canberra, Australia, and Monash University, Melbourne, Australia, for pancreas harvest and islet isolation and as recipients of islet transplants. All experiments performed with mice were approved by the Australian National University Animal Experimentation Ethics Committee.

Cell Lines

The PFHR-9 cell line, derived from a mouse embryonal carcinoma, was obtained from Professor Erik Thompson (St Vincent's Institute of Medical Research, Melbourne, Australia) and maintained in culture in Dulbecco's modified Eagle medium (DMEM) supplemented with 25 mM glucose (Cat. No. 11995; Gibco/Invitrogen, Carlsbad, CA, USA), 10% fetal calf serum (SAFC Biosciences, Bunbury, Western Australia, Australia), and antibiotics [penicillin G (Cat. No. 156065; MP Biomedicals, Santa Ana, CA, USA), streptomycin sulfate (Cat. No. S6501; Sigma-Aldrich, St. Louis, MO, USA), neomycin sulfate (Cat. No. N-6386; Sigma-Aldrich)] in a humidified gas phase of 5% CO_2 in air. Adherent PFHR-9 cells were harvested using 0.05% ethylenediaminetetraacetic acid (EDTA; Cat. No. 10093.5V; BDH Chemicals, Kilsyth, Victoria, Australia) and transferred to individual wells of CELLSTAR 96-well plates (Greiner Bio-one, Frickenhausen, Germany) at 2×10^5/well for intracellular staining of matrix proteins and analysis by flow cytometry.

Islet Isolation

Islets were isolated as previously described (9,46). Briefly, islets were isolated from groups of five anesthetized donor CBA or C57BL/6 mice {0.025 ml Avertin/g body weight [70 mM 2,2,2-tribomoethanol; Cat. No. T48402, Sigma-Aldrich, in 2% (v/v) 2-methyl-2-2 butanol; Fluka Chemie AG, Buch, Switzerland]} by initially perfusing the pancreas in situ via the common bile duct with 2.5 mg/ml of collagenase P (Roche Diagnostics,

Mannheim, Germany). The inflated pancreas was digested further with an additional 2.5 mg/ml of collagenase P in a stationary water bath at 37°C. The digest was then shaken briefly by hand, vortexed lightly, placed on ice to terminate enzymatic digestion, and washed. Islets were handpicked from the digested pancreas tissue with the aid of a dissecting microscope (Kyowa Optical SDZ-P, Tokyo, Japan). Isolated islets were either immediately frozen in liquid Forane® refrigerant preequilibrated in liquid nitrogen (134a; Arkema Inc., King of Prussia, PA, USA) or transplanted.

β-*Cell Isolation*

CBA mouse islets were dispersed into single-cell suspensions using 1 mg/ml Dispase II (Roche) in chelation buffer, as previously described (57). Islet β-cells ($3–4\times10^4$) were transferred to individual wells of CELLSTAR 96-well plates (Greiner Bio-one) in Roswell Park Memorial Institute (RPMI) 1640 medium (Gibco/Invitrogen) supplemented with 10% fetal calf serum for immunofluorescence staining of matrix proteins and analysis by flow cytometry.

Islet Transplantation

Islets prepared from CBA donors were transplanted as isografts and allografts to CBA and C57BL/6 recipient mice, respectively; C57BL/6 islets were also transplanted to C57BL/6 and CBA mice as isografts and allografts, respectively. To aid transplantation, isolated mouse islets were embedded in blood clots prepared from the recipient mouse strain's blood (50–100 adult islets per clot, 250 islets per transplant). The islets contained in blood clots (three clots per graft) were transplanted beneath the kidney capsule of recipient mice anesthetized with Avertin (0.012 ml/g body weight intraperitoneally), as previously described (45,46). Transplant recipients were killed by cervical dislocation at 3, 5, 7, or 10 days posttransplant. Grafts were frozen in liquid Forane 134a (preequilibrated with liquid nitrogen), embedded in OCT compound (Cat. No. 1A018; ProSciTech, Thuringowa, Queensland, Australia), and stored at −70°C until frozen sectioning and staining.

Immunofluorescence Staining of Tissue Sections and Analysis by Microscopy

Immunohistochemistry was performed as previously described (17). Tissue sections (10 μm) were prepared using a CM1800 Leica cryostat (Adeal, Altona North, Victoria, Australia), collected on Superfrost glass slides (HD Scientific Supplies, Glengala, Victoria, Australia), and stored at −20°C until use. The antibodies used for immunohistochemistry and the relevant fixation conditions are summarized in Table 1. Unfixed sections were dried under vacuum for 5 min, followed by fixation in either formalin (Cat. No. FO00112500; Chem-Supply Pty Ltd, Gillman, South Australia, Australia) or 100% ethanol (Cat. No. EA043-10L-P; Chem-Supply Pty Ltd) (Table 1). Sections were then rinsed in 3×5-min changes of hypertonic phosphate-buffered saline [10 mmol/L sodium/potassium phosphate (Cat. No. P5379; Sigma-Aldrich Pty Ltd, Castle Hill, New South Wales, Australia) with 0.274 mol/L NaCl [Cat. No. 131659.1214; Panreac/Pure Science Ltd, Plimmerton, Porirua, New Zealand] and 5 mmol/L KCl (Cat. No. 383; Ajax Finechem Pty Ltd, Seven Hills, New South Wales, Australia); pH 7.2] before treatment with blocking solution (10% v/v normal donkey serum; Sigma-Aldrich) in antibody diluent containing 0.55 mol/L NaCl and 10 mmol/L sodium phosphate (Monobasic: Cat. No. S8282, Dibasic: Cat. No. S7907; Sigma-Aldrich Pty Ltd; pH 7.1) for 20 min at room temperature. Incubation with primary antibodies was carried out overnight at room temperature. Secondary antibodies (Jackson ImmunoResearch Laboratories, West Grove, PA, USA) used to localize components of Engelbreth–Holm–Swarm tumor (EHS) laminin 111 and nidogen-2 were donkey anti-rabbit IgG conjugated to fluorescein (1:100; Cat. No. 711-096-152) and cyanine 3 (Cy3; 1:100; Cat. No. 711-166-152), respectively. For detecting dual

Table 1. Primary Antibodies and Fixation Conditions Used for Immunoflourescence Staining

	Primary Antibody				
Antigen (Species)	Host Species	Code	Source	Dilution	Fixation
Laminin α2 (mouse)	Rat	4H8-2	Sigma Chemical, Castle Hill, NSW, Australia	1:3200	Formalin
Type IV collagen (mouse)	Rabbit	T40263R	Biodesign, Meridian Life Science, Memphis, TN, USA	1:100	Formalin
Laminin EHS (mouse)	Rabbit	L9393	Sigma Chemical	1:100	100% Ethanol
Nidogen-2 (mouse)	Rabbit	Ab14513	Abcam, Cambridge, UK	1:800	Formalin
Perlecan (mouse)	Rabbit	906	Dr. Dziadek[a] (8)	1:800	100% Ethanol
PECAM-1/CD31	Rat	390	BD Pharmingen/BD Bioscience, North Ryde, NSW, Australia	1:500	100% Ethanol

[a]M. Dziadek, Garvan Institute of Medical Research, Darlinghurst, NSW, Australia.
EHS, Engelbreth–Holm–Swarm tumor; PECAM-1/CD31, platelet endothelial cell adhesion molecule-1/cluster of differentiation 31.

localizations of laminin α2 and collagen type IV, and perlecan and platelet endothelial cell adhesion molecule-1 (PECAM-1), secondary antibodies were donkey anti-rat IgG conjugated to Cy3 (1:100; Cat. No. 715-165-153) and biotin-SP-conjugated Affinipure donkey anti-rabbit IgG followed by fluorescein-conjugated streptavidin (1:100; Cat. No. 016-090-084). Sections were treated with 100 μM 4′,6-diamidino-2-phenylindole dihydrochloride (DAPI) (Molecular Probes, Eugene, OR, USA) to identify nuclei, and coverslips (Cat. No. HDLD22401-01P0; HD Scientific Supplies Pty Ltd, Wetherill Park, New South Wales, Australia) were attached with mounting medium for fluorescence microscopy (Dako Corporation, Carpinteria, CA, USA). Sections were observed and photographed with an Olympus BX50 microscope with an epifluorescence attachment and a Spot RT digital camera (Diagnostic Instruments, Sterling Heights, MI, USA). For light microscopy, frozen sections were fixed in formalin and stained with hematoxylin and eosin (H&E) (Cat. No. GHS232 and HT11033; Sigma-Aldrich Pty Ltd.).

Flow Cytometry

For intracellular staining, isolated β-cells (prepared from islets harvested from groups of five donor mouse pancreases) and PFHR-9 cells were first fixed and permeabilized using the BD Cytofix/Cytoperm Fixation/Permeabilization Kit (BD Pharmingen/BD Biosciences, San Jose, CA, USA). The cells were then stained with polyclonal rabbit anti-EHS laminin (Sigma-Aldrich), anti-mouse collagen type IV (AbD Serotec, Kidlington, Oxfordshire, UK), anti-mouse nidogen-2 (Abcam, Cambridge, UK), or anti-mouse perlecan (Dr. Dziadek, Sydney, Australia), followed by phycoerythrin (PE)-donkey anti-rabbit IgG (Jackson ImmunoResearch, West Grove, PA, USA). Rabbit IgG (Southern Biotech, Birmingham, AL, USA) was used as the isotype control IgG. The geometric mean fluorescence ratio (GMFR) was calculated by dividing the geometric mean fluorescence intensity (GMFI) of cells stained with primary antibody by the GMFI of cells stained with the isotype control IgG (57). Cells were analyzed using a BD LSRI flow cytometer and CellQuest™ software (version 6.0, BD Biosciences).

RESULTS

Localization of BM Matrix Proteins in Islets In Situ and In Vitro

Immunofluorescence staining of normal CBA islets in situ in the pancreas (Figs. 1–3), as previously reported for insulitis-free nonobese diabetic (NOD)/Lt islets (17), confirmed that a continuous islet BM consisting of perlecan (Fig. 1A), collagen type IV (Fig. 1B), laminin α2 (Fig. 1B), components of EHS laminin 111 (Fig. 2C), and nidogen-2 (Fig. 2D) was localized at the islet periphery. These studies further indicated that laminin α2 was more

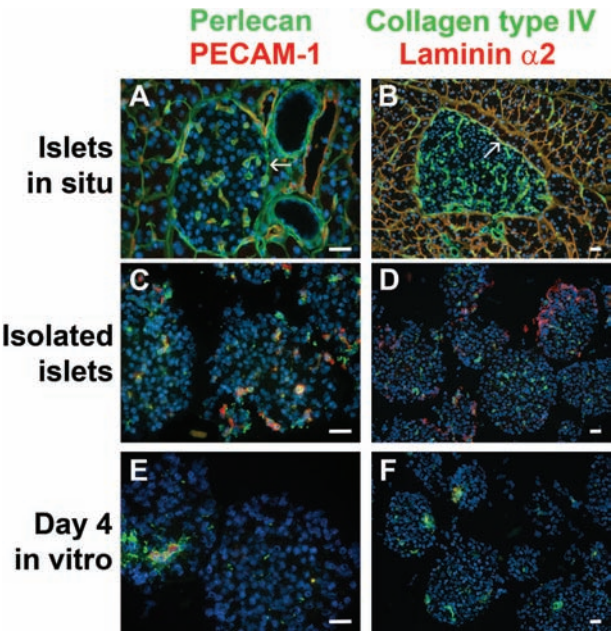

Figure 1. Pancreatic islet basement membrane (BM) is lost during islet isolation and does not recover after in vitro culture. CBA mouse islets in situ in the pancreas (A, B), freshly isolated (C, D), or after 4 days in vitro culture (E, F) were examined by immunofluorescence microscopy for their content and distribution of perlecan (green fluorescence), platelet endothelial cell adhesion molecule-1 (PECAM-1; red fluorescence), collagen type IV (green fluorescence), and laminin α2 (red fluorescence). Yellow fluorescence represents sites where green and red fluorescence colocalize. The islet BM in situ in A and B is identified by peri-islet staining for perlecan, collagen type IV, and laminin α2 (arrows). Colocalization of perlecan and PECAM-1 identified some subendothelial BM at the islet periphery and within the islets in situ in the pancreas (A). Nuclei are counterstained blue with 4′,6-diamidino-2-phenylindole dihydrochloride (DAPI). Arrows indicate location of islet BM. Scale bars: 25 μm.

strongly associated with the BM of pancreatic acini than with the islet BM (Fig. 1B). Because a double BM has previously been reported for the intraislet blood vessels of human islets but not mouse islets (53), colocalization of perlecan with PECAM-1-positive VECs of intraislet capillaries and peri-islet blood vessels was identified as the subvascular endothelial BM (Fig. 1A). This vascular endothelial BM also stained strongly for collagen type IV (Fig. 1B), components of EHS laminin 111 (Fig. 2C), and nidogen-2 (Fig. 2D) but showed weak localization of laminin α2 (Fig. 1B).

In contrast to islets in situ, freshly isolated CBA islets in vitro revealed substantial damage to the islet BM, with loss of perlecan (Fig. 1C), collagen type IV (Fig. 1D), components of EHS laminin 111 (Fig. 2G), and nidogen-2 (Fig. 2H) and extensive disruption of laminin α2 (Figs. 1D and 2F). In contrast, residual intraislet vascular BM was characterized by retention of perlecan (Fig. 1C), collagen type IV (Fig. 1D), EHS laminin (Fig. 2G), and nidogen-2

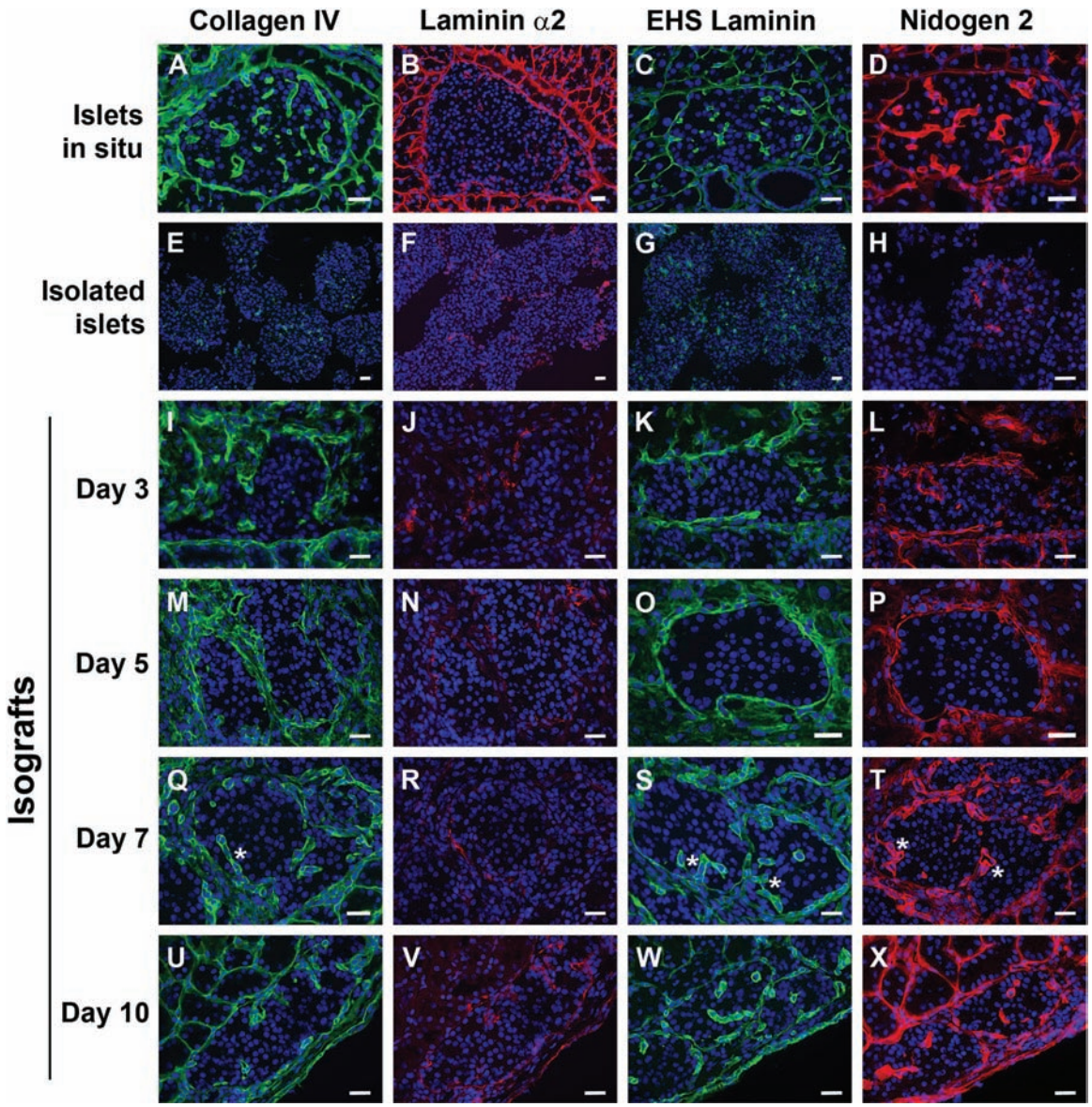

Figure 2. Complete reconstitution of the islet BM occurs over a 10-day period in islet isografts transplanted under the kidney capsule. Collagen type IV, laminin α2, components of Engelbreth–Holm–Swarm tumor (EHS) laminin 111, and nidogen-2 were localized by immunofluorescence staining in CBA islets in situ in the pancreas (A–D), CBA isolated islets (E–H), and in CBA islet isografts at day 3 (I–L), day 5 (M–P), day 7 (Q–T), and day 10 (U–X) posttransplant. Nuclei are counterstained blue with DAPI. M and N, Q and R, and U and V show dual localization of collagen type IV and laminin α2, respectively, whereas K and L, O and P, and S and T show localization of components of EHS laminin 111 and nidogen-2 on adjacent sections. *Invaginations into the islets. Scale bars: 25μm.

(Fig. 2H) but little, if any, laminin α2 (Fig. 1D). There was no evidence of recovery of the islet BM during in vitro culture of the islets for 4 days (Fig. 1E, F), and the lumen of intraislet capillaries, which was characteristic of freshly isolated islets (Fig. 1C, D), was no longer clearly evident. Instead, there appeared to be isolated and diffuse staining for matrix proteins within the islets (Fig. 1E, F) associated with residual PECAM-1$^+$ VECs (Fig. 1E). This finding raised the possibility that in vitro, surviving intraislet endothelial cells were secreting matrix proteins de novo. The islet BM also failed to be restored in vitro after prolonged culture of the islets for 7 days (data not shown). However, central necrosis, which was more prominent within the islets after 7 days of culture, compared with 4-day cultured islets, indicated a deterioration in islet viability.

Recovery of Peri-Islet BM and Intraislet Vascular BM After Islet Isotransplantation

Unlike isolated CBA islets (Figs. 1C, D; 2E–H; and 3D–F) and islets maintained in culture (Fig. 1E, F),

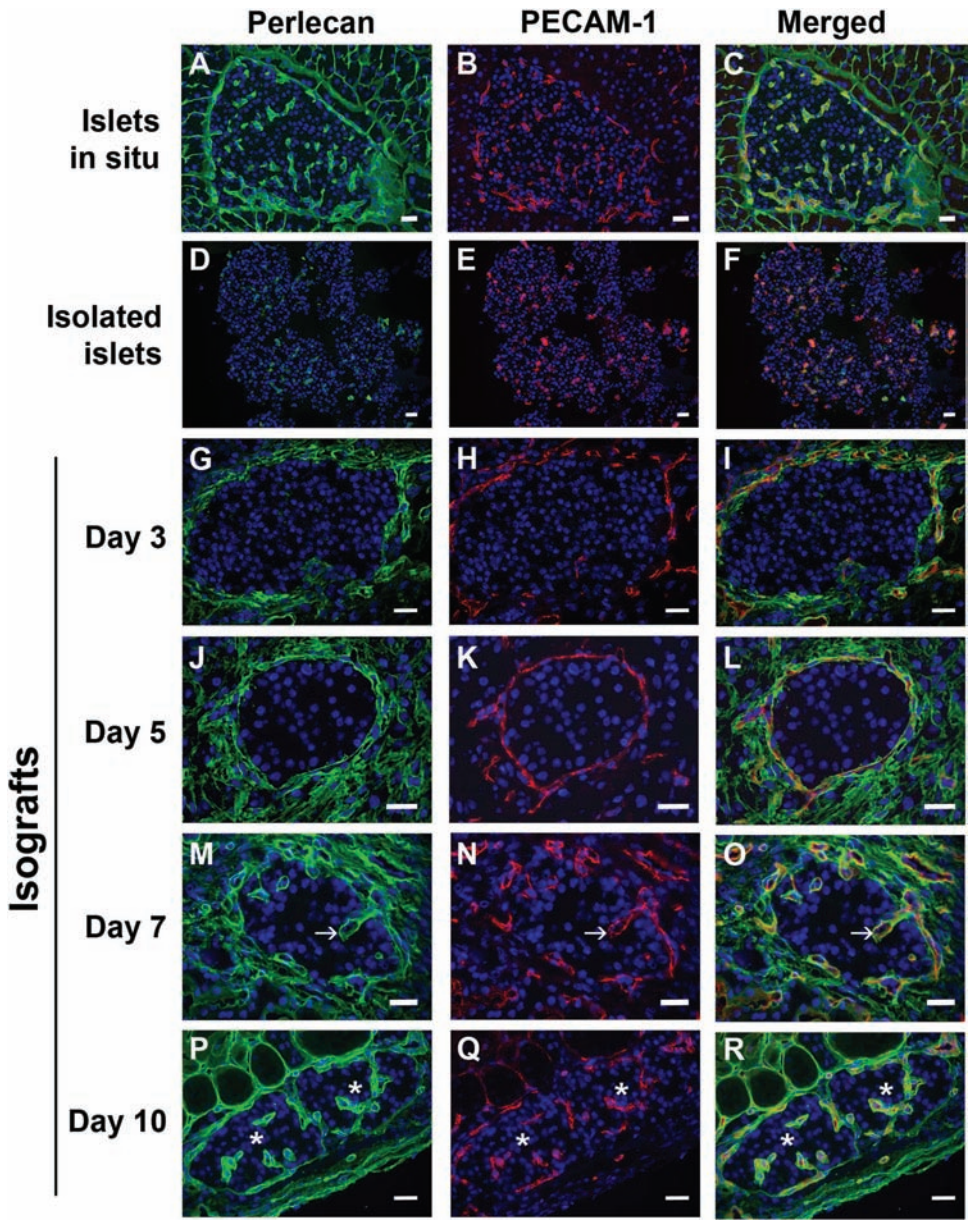

Figure 3. Recovery of the islet BM after transplantation and revascularization of the engrafted islets correlates with the migration of PECAM-1$^+$ VECs. CBA islets in situ in the pancreas (A–C), CBA isolated islets (D–F), and CBA islet isografts at day 3 (G–I), day 5 (J–L), day 7 (M–O), and day 10 (P–R) posttransplant were analyzed by fluorescence staining for the localization of perlecan and the endothelial cell marker PECAM-1. Merged images of perlecan (A, D, G, J, M, P) with PECAM-1 (B, E, H, K, N, Q), respectively, are also shown (C, F, I, L, O, R). Recovery of peri-islet perlecan at 3–5 days after transplantation (G, J) correlated with continuous peri-islet expression of PECAM-1 (H, K). Perlecan (M, P) and PECAM-1 (N, Q) staining coinvaginated into the engrafted islets by 7–10 days posttransplant (arrows in M, N, O and asterisks in P, Q, R). Although continuous peri-islet PECAM-1 staining had disappeared by day 7 posttransplant (N), uninterrupted peri-islet perlecan staining remained at 7–10 days (M, P), representing the newly formed islet BM. Nuclei are counterstained blue with DAPI. Scale bars: 25 μm.

isogeneic CBA islets engrafted beneath the kidney capsule of CBA recipient mice [which do not mount a rejection response due to the cells being genetically identical to the donor islets at both the major histocompatibility complex (MHC) and non-MHC loci] exhibited recovery of the islet BM. Deposition of collagen type IV (Fig. 2I), laminin $\alpha 2$ (Fig. 2J), EHS laminin (Fig. 2K), nidogen-2 (Fig. 2L), and perlecan (Fig. 3G) was evident at day 3 posttransplant, but the staining was incomplete and often diffuse around the periphery of the islets. Staining of

matrix proteins at 5 to 7 days posttransplant revealed further peri-islet remodeling and organization (Fig. 2M, O–Q, S, T; Fig. 3J, M) with the exception of laminin α2 (Fig. 2N, R), which reappeared more slowly. At day 7 posttransplant, collagen type IV, components of EHS laminin 111 and nidogen-2 were localized within the islets and appeared to be invaginations from the islet periphery (Fig. 2Q, S, T). By day 10, the peri-islet BMs showed complete reconstitution with continuous staining for the proteins, collagen type IV (Fig. 2U), laminin α2 (Fig. 2V), components of EHS laminin 111 (Fig. 2W), nidogen-2 (Fig. 2X), and perlecan (Fig. 3P).

In parallel with the disorganized deposition of BM matrix proteins at the periphery of engrafted islets on day 3, we observed discontinuous peri-islet staining for PECAM-1 (a marker for VECs), suggesting that VECs had migrated to peri-islet sites (Fig. 3H). The intraislet localization of perlecan (Fig. 3G) at day 3 also correlated with localization of intraislet staining for PECAM-1 (Fig. 3H, I), defining vascular endothelial BM that may have been derived from the isolated donor islets (Fig. 3D, E). The colocalization of perlecan and PECAM-1 staining, which was continuous around the periphery of islets by day 5 (Fig. 3J, K, L), strongly suggested that the BM matrix proteins may have been secreted by nearby VECs. From day 7, the PECAM-1$^+$ VECs (Fig. 3N) with associated perlecan$^+$ BM (Fig. 3M) were found to invade the islet cell mass, suggesting the formation of intraislet blood vessels (Fig. 3O). This process was accompanied by interruption of the peri-islet PECAM-1 staining (Fig. 3N). By day 10, perlecan staining showed both peri-islet and intraislet BM localization (Fig. 3P); however, costaining with PECAM-1 was restricted only to intraislet vascular endothelial BM (Fig. 3Q, R). Importantly, at this point, the preserved peri-islet staining for perlecan (Fig. 3P) at day 10, as well as for collagen type IV (Fig. 2U), laminin α2 (Fig. 2V), and components of EHS laminin 111 (Fig. 2W) and nidogen-2 (Fig. 2X), characterized the complete recovery of the islet BM and resembled the islet BM in situ in the pancreas (Figs. 1A, B; 2A–D; and 3A). These findings indicate that full recovery of the islet BM of transplanted islets occurs by 10 days after transplantation.

Islet β-cells Do Not Produce BM Matrix Proteins

To further determine the source of ECM proteins that form the islet BM, we investigated by flow cytometry whether β-cells isolated from CBA islets produced matrix proteins (Fig. 4). Matrix-producing PFHR-9 cells showed strong intracellular staining for components of EHS laminin 111 (mean GMFR, 29.1 ± 4.0) (Fig. 4A), collagen type IV (mean GMFR, 7.5 ± 0.9) (Fig. 4B), perlecan (mean GMFR, 6.9 ± 0.6) (Fig. 4D) but stained weakly for nidogen-2 (mean GMFR, 1.7 ± 0.4) (Fig. 4C). These same matrix proteins were not detected in isolated β-cells above background levels obtained with isotype control IgG (GMFRs ~1) (Fig. 4A–D).

The Status of Islet and Vascular Endothelial BMs in Islet Allografts During Rejection

Figure 5 shows that compared with islet isografts, which consisted of intact islet tissue (Fig. 5A, G, P), islet allografts showed peri-islet accumulation of host MNCs by 5 days (Fig. 5M) and intraislet MNC invasion by 7 days (Fig. 5S). Like CBA and C57BL/6 islet isografts at day 3 (Fig. 3G–I and Fig. 5B, C, respectively), peri-islet deposition of perlecan correlated with localization of PECAM-1$^+$ VECs in CBA islet allografts at 3 days after transplantation to C57BL/6 recipient mice (Fig. 5E, F). The peri-islet and intraislet staining for perlecan in islet allografts at day 5 (Fig. 5K) resembled the corresponding islet isografts (Fig. 5H), with the exception of prominent perlecan-positive vessel-like structures at the islet periphery in islet allografts (Fig. 5K), suggesting the formation of peri-islet blood vessels. However, the staining for PECAM-1 differed markedly between iso- and allografts at day 5 (Fig. 5I, L, O) and day 7 (Fig. 5R, U). Whereas C57BL/6 islet isografts showed predominantly peri-islet PECAM-1 staining as well as intraislet staining (Fig. 5I), peri-islet PECAM-1 staining within islet allografts was weak (Fig. 5L) or less prominent (Fig. 5O). The decline in PECAM-1 expression correlated with the local accumulation of MNCs at the graft site (Fig. 5M). Patent peri-islet blood vessels containing MNCs were evident at day 5 (Fig. 5M–O) and day 7 (Fig. 5S–U), but intraislet vasculature was not identified (Fig. 5L, O, U). Islets damaged by MNC infiltration at day 7 also exhibited peri-islet perlecan staining, which correlated with PECAM-1-positive VECs. In addition, diffuse staining for perlecan was localized at extraislet sites for both iso- and allografts (Fig. 5H, K, Q) and is consistent with the extraislet deposition of collagen type IV and EHS laminin (Fig. 2M, O) within the graft site. These findings indicate that after islet allotransplantation, assembly of a VEC-derived BM at the periphery of engrafted islets is initiated but the formation of intraislet blood vessels fails to occur. Although there is evidence for the formation of a peri-islet BM before intraislet MNC invasion (Fig. 5N), it is unclear from this allograft model whether a continuous BM around the islets is established before islet destruction occurs. In any case, the deposition of the BM matrix protein perlecan within the graft site stroma of islet allografts suggests the formation of an ad hoc BM-like barrier to cell migration.

To further explore the temporal relationship between peri-islet BM assembly and MNC infiltration into engrafted islets during allograft rejection, we analyzed allografts generated from the reverse donor and recipient mouse strain combination, where C57BL/6 islets transplanted into CBA recipient mice are rejected at a slower tempo (Fig. 6). By days 5–7, continuous peri-islet staining

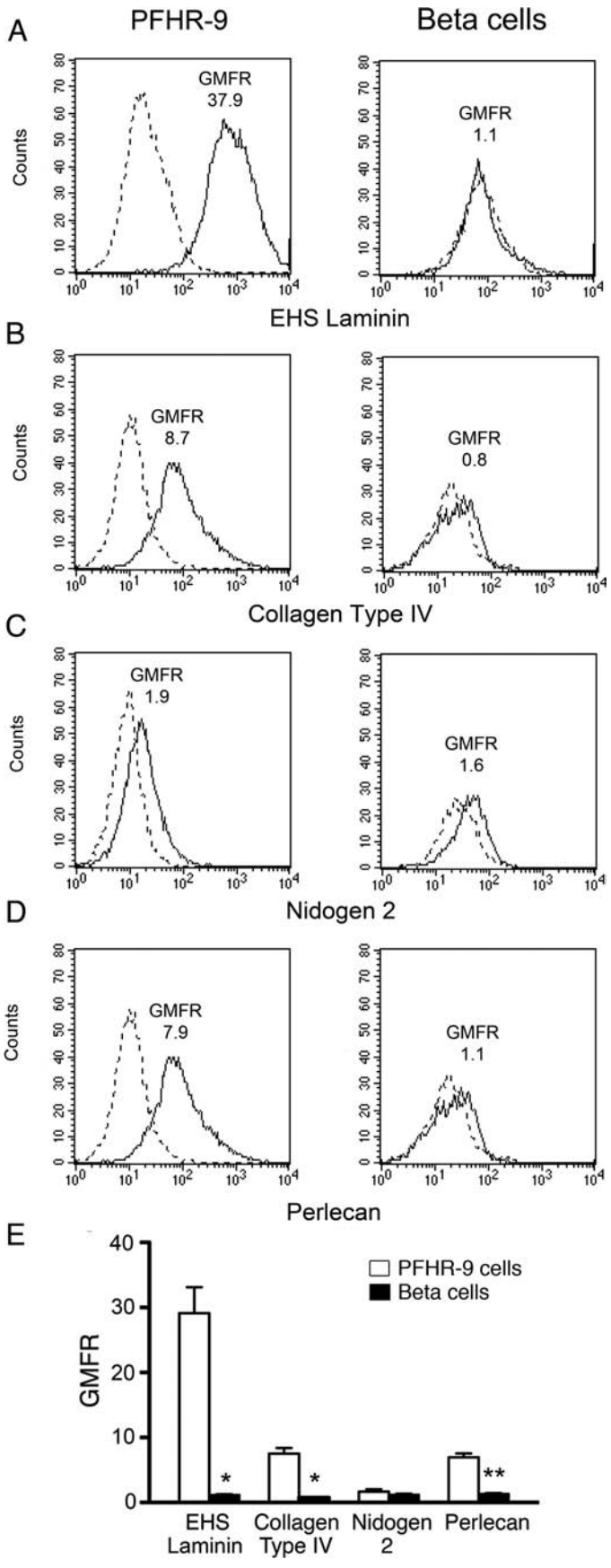
A
PFHR-9
Beta cells
Counts
GMFR
37.9
GMFR
1.1
EHS Laminin
B
GMFR
8.7
GMFR
0.8
Collagen Type IV
C
GMFR
1.9
GMFR
1.6
Nidogen 2
D
GMFR
7.9
GMFR
1.1
Perlecan
E
PFHR-9 cells
Beta cells
GMFR
EHS Laminin
Collagen Type IV
Nidogen 2
Perlecan

for perlecan (Fig. 6B, F) was accompanied by peri-islet localization of PECAM-1 (Fig. 6C, G), suggesting that formation of a peri-islet BM was in progress. This feature correlated with a protracted rejection response and preservation of intact islet tissue. In addition, like CBA islet allografts in C57BL/6 recipient mice (Fig. 5K, L, N, O, T, U), the islets often showed vascular BM surrounding an expanded lumen (Fig. 6D), possibly reflecting enlarged blood vessels servicing the allograft inflammatory response, but intraislet vasculature was absent (Fig. 6B–D). Substantial perlecan and PECAM-1 staining was also observed throughout the graft site stroma (Fig. 6B–D, F–H), with an intense MNC infiltrate present by day 7 (Fig. 6E). In this islet allograft model, formation of a complete VEC-derived peri-islet BM appeared to be established in islets before the onset of intraislet MNC invasion and islet destruction. Nevertheless, the lack of intraislet blood vessels and the presence of prominent peri-islet vasculature were found to be consistent features of engrafted allogeneic islets facing imminent rejection at 5–7 days posttransplant.

DISCUSSION

This study clearly confirms that the islet BM of normal mouse islets present in situ in the pancreas and characterized by the localization of collagen type IV, laminins (components of 111 and α2), nidogen-2, and perlecan (17) is destroyed during the enzymatic isolation of islets in vitro, with only remnants of laminin α2 remaining at the periphery of the islets (Fig. 1). Although some residual BM of intraislet capillaries was evident in freshly isolated islets, the islets continued to lose much of their intraislet vascular BM during 4 days of culture. Despite this, residual PECAM-1$^+$ VECs were found adjacent to scattered sites of diffuse staining for intraislet perlecan. This finding is consistent with previous studies demonstrating matrix protein production by VECs in situ (27,28) and the substantial loss of intraislet VECs during culture (29). Nevertheless, the islet BM did not recover in vitro because no peri-islet staining for perlecan, collagen type IV, or laminin α2 was observed after maintaining the islets in culture for either 4 days (Fig. 1) or 7 days. This finding is in disagreement with a previous report that islets regain their BM in culture, as assessed by the reappearance of reticulin staining around the islet periphery (54). We attribute this different interpretation to the lack of specificity of silver-based reticulin staining for BM matrix proteins and the more likely detection of a fibroblast capsule around the islets using this approach (3,39).

We found that the islet BM was reestablished in vivo after islet transplantation. Assembly of a peri-islet BM was well underway by as early as 3 days posttransplant and was characterized by prominent, discontinuous staining for collagen type IV, components of EHS laminin 111, nidogen-2, and perlecan (Figs. 2 and 3). Continuity of the peri-islet BM staining was generally established by 5 days posttransplantation (Figs. 2 and 3) but uninterrupted peri-islet laminin α2 staining was not established until day 10 (Fig. 2), by which time the peri-islet BM had undergone further remodeling, with the staining profile of the engrafted islets resembling islets in situ in the pancreas. Flow cytometry analyses of isolated islet β-cells failed to detect intracellular levels of BM matrix proteins (Fig. 4), thereby ruling out the islet cells as the source of ECM proteins for BM recovery. Instead, peri-islet deposition of BM matrix proteins coincided with the localization of PECAM-1-positive VECs that had migrated to the periphery of the islets (Fig. 3) by 3–5 days posttransplant. At 5 days, in particular, the peri-islet staining for collagen type IV, components of EHS laminin 111, nidogen-2, and perlecan was widespread and extended beyond the islet boundary into the surrounding stroma of the graft site. Together, these findings suggested that the peri-islet BM matrix proteins were most likely secreted by the VECs, a recognized property of VECs (27,28). Molecular remodeling of the ECM proteins could then lead to the formation of a peri-islet BM resembling a protective "shell" around the islets. From 7 to 10 days posttransplant, the PECAM-1 staining no longer coincided with the peri-islet BM and instead colocalized with intraislet BM, consistent with the migration of VECs into the islets and with the formation of intraislet vascular endothelium. The separation of the peri-islet BM and PECAM-1$^+$ VECs marked the reestablishment of the independent islet BM, albeit most likely VEC-derived, and probably represents another example of how migrating or regressing VECs can abandon the BM that they deposit (24,28).

The origin of the VECs potentially responsible for the recovery of the islet BM is unclear. An isolated region of VECs and subendothelial BM was identified within some engrafted islets as early as 3 days posttransplant (Figs. 2 and 3) but was not observed by 5 days, suggesting

FACING PAGE

Figure 4. Isolated islet β-cells do not produce BM matrix proteins. Intracellular staining for BM matrix proteins was assessed by flow cytometry in control mouse embryonal carcinoma (PFHR-9) cells (A–E) and in isolated CBA islet β-cells (A–E). The solid line in A to D shows the staining with primary rabbit anti-mouse (A) EHS laminin, (B) collagen type IV, (C) nidogen-2, and (D) perlecan polyclonal antibody (pAb), and the dotted line shows the background staining obtained with an isotype control rabbit IgG. The data in (E) show the mean GMFR ± SEM for EHS laminin, collagen type IV, nidogen-2, and perlecan staining in β-cells and PFHR-9 cells from $n = 4$–5 independent experiments. *$p = 0.0079$; **$p = 0.0286$, compared with control PFHR-9 cells.

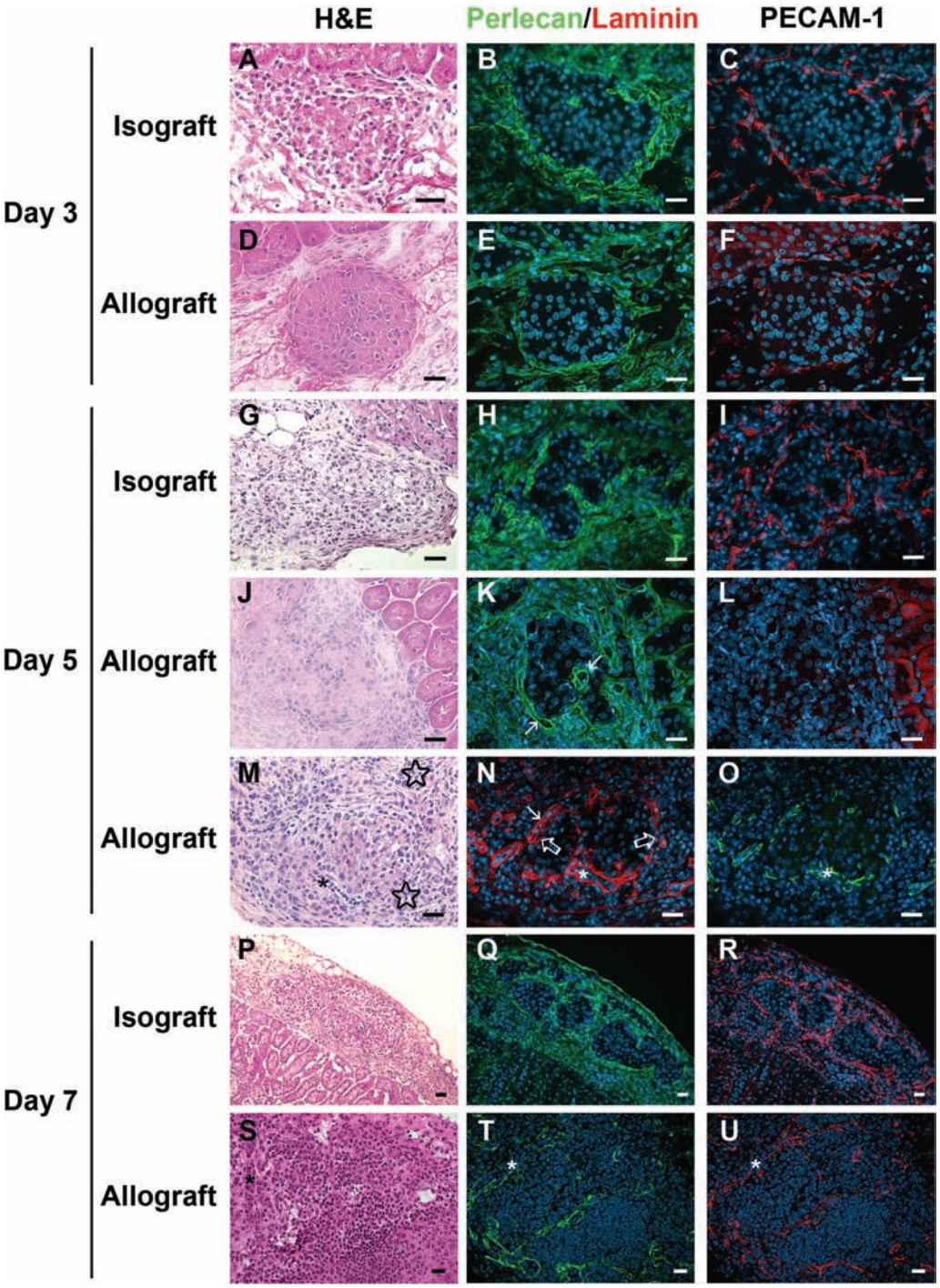

Figure 5. Recovery of peri-islet BM perlecan occurs without the formation of intraislet blood vessels in rejecting islet allografts. C57BL/6 islet isografts and CBA islet allografts in C57BL/6 recipient mice at 3–7 days after transplantation beneath the kidney capsule were examined by dual immunofluorescence staining of sections for perlecan (B, E, H, K, Q, T) and PECAM-1 (C, F, I, L, R, U), and laminin (N) and PECAM-1 (O). H&E-stained serial sections of immunolabeled islets are also shown (A, D, G, J, M, P, S). Host mononuclear cells (MNCs) were found to accumulate around intragraft islets by 5 days (M, region indicated by stars) and were present in prominent vessel lumens at the periphery of islets (asterisk in M–O, S–U). Arrows indicate prominent blood vessels; open arrows indicate the peri-islet BM. Nuclei are counterstained blue with DAPI. Scale bars: 25μm.

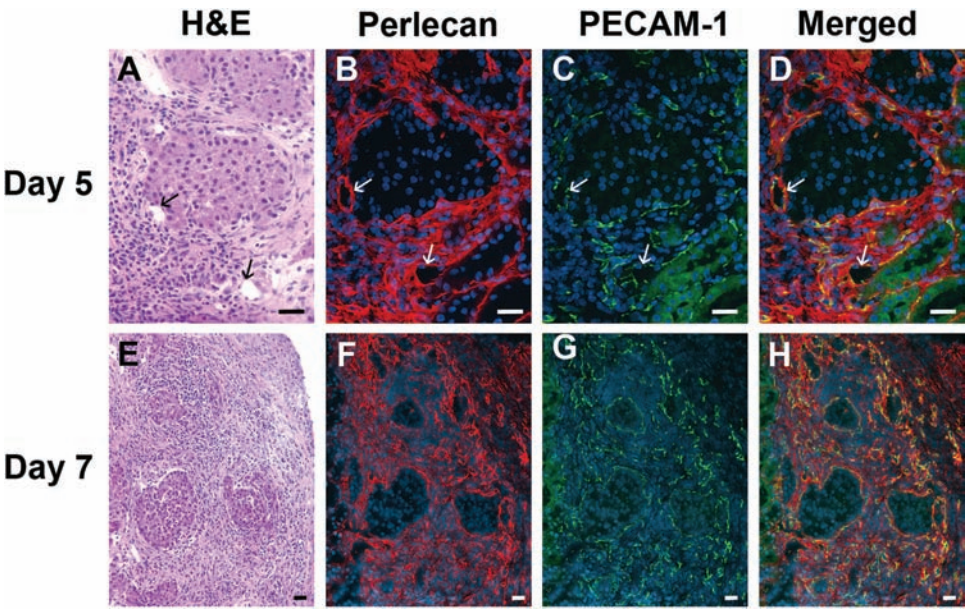

Figure 6. Reestablishment of peri-islet BM perlecan is accompanied by peri-islet migration of PECAM-1$^+$ endothelial cells in rejecting islet allografts. C57BL/6 islet allografts at 5 (A–D) and 7 (E–H) days posttransplant to CBA mice were analyzed by immunofluorescence staining for perlecan (red fluorescence) and PECAM-1 (green fluorescence). The merged images show yellow fluorescence, revealing the colocalization of perlecan and PECAM-1 staining around the periphery of islets. Arrows identify enlarged peri-islet blood vessels. Perlecan staining is also strongly expressed and diffusely distributed throughout the graft site (B, F). H&E-stained serial sections (A, E) of the immunostained islets reveal the presence of intact islet tissue, despite an intense MNC infiltrate at the graft site. Nuclei are counterstained blue with DAPI. Scale bar: 25 μm.

that these intraislet VECs may have migrated to the islet periphery. However, other studies have reported that transplanted islets are revascularized predominantly by endothelium of recipient origin (7,25,52), with donor-type VECs remaining after islet isolation, also contributing to the process (5,19,29). β-Cells produce vascular endothelial growth factor (VEGF-A) (7), which could recruit host VECs to the graft site and to the periphery of transplanted islets (22). It is therefore possible that both host and residual donor VECs play a critical role in repairing the BMs of engrafted islets.

The matrix detachment of islet cells resulting from loss of the islet BM during islet isolation and the quick onset of the islet BM recovery process in vivo after transplantation is offset to some extent by a staggered loss of intraislet vasculature after islet isolation and a relatively slow process of islet revascularization. This asynchrony between the loss and recovery of the peri- and intraislet BMs may ensure that islet cells are not completely devoid of matrix attachment during engraftment, a property that would promote β-cell survival. Nevertheless, we have observed that the BM remodeling process proceeds over a period of 7 to 10 days, suggesting that at least some matrix detachment-induced β-cell apoptosis (41,50,51,55) is likely. This would be expected to compound the β-cell apoptosis induced by loss of intracellular heparan sulfate in the β-cells during islet isolation (57). Our findings therefore support the notion of cotransplanting VEC/mesenchymal stem cell (MSC) mixtures (20) with isolated islets, not only to facilitate more rapid revascularization of the engrafted islets (6) to actively provide nutrients and oxygen for β-cell metabolism and function but also to more promptly establish peri- and intraislet BM recovery and matrix reattachment. The restoration of β-cell–matrix interactions would be expected to provide major benefits to islet survival and function, as previously demonstrated in vitro (13,21,27,34,56) and in vivo (42), and to minimize primary islet loss in a transplant setting.

In the situation of islet allotransplantation, we found that, initially, the remodeling of the peri-islet BM, as revealed by perlecan localization, resembled the pattern for islet isografts (Fig. 5). However, in contrast to the peri-islet PECAM-1$^+$ staining observed at 3 days after allotransplantation, very little peri-islet PECAM-1 staining was observed at 5–7 days in the CBA to C57BL/6 mouse strain combination in which aggressive islet destruction by infiltrating MNCs occurs because of allograft rejection (Fig. 5). In comparison, peri-islet PECAM-1 staining was observed at 7 days in the reverse C57BL/6 to CBA mouse strain combination where islet destruction is routinely delayed because of a slower tempo of rejection (Fig. 6). Indeed, this low level of PECAM-1 staining is probably due to the

downregulation of PECAM-1 expression by cytokines produced by nearby invading MNCs, as previously reported (26,49), and to mouse strain-specific effects, rather than the loss of VECs. A striking difference between the isograft (Figs. 3 and 5) and allograft (Figs. 5 and 6) models, however, with both mouse strain combinations, was the consistent lack of intraislet vascular BMs in the allografts by day 7. Instead, the allografts were characterized by an abundance of peri-islet and intragraft perlecan$^+$ BMs (Figs. 5 and 6) and the colocalization of PECAM-1$^+$ endothelial cells (Fig. 6), consistent with increased vascularization of the graft site during rejection. Indeed, the profuse peri-islet vasculature was found to contain nucleated DAPI$^+$ cells, consistent with the delivery of MNCs to the engrafted islets (Fig. 5N, O, T, and U). Together, these findings suggest that although VECs initially commence the deposition of peri-islet BMs in islet allografts, the cue for the formation of intraislet vasculature fails to occur, and instead, VECs are diverted to enhance the peri-islet and intragraft vasculature required to transport activated alloreactive T cells to the engrafted donor islet tissue. The factors that regulate this change may involve inflammatory cytokines (32) and/or chemokines (48). In the context of an allograft rejection response, it is likely that such VECs would be of host origin and that the increased peri-islet vasculature and vasodilation could facilitate MNC delivery to the transplanted islets, as previously described for sites of acute inflammation (38). In contrast to islet isografts, we therefore predict that in an allograft setting without adequate immune protection, the cotransplantation of exogenous VECs/MSCs to facilitate islet revascularization (20) may well induce the undesired effect of accelerating allograft rejection.

We propose that the effector mechanisms required by infiltrating MNCs to enter engrafted allogeneic islets are likely to be substantially influenced by the presence or absence of an islet BM. We have previously reported that insulitis MNCs critically require the heparan sulfate-degrading enzyme heparanase to solubilize and traverse the islet BM in NOD/Lt islets in situ to initiate destructive insulitis and the development of autoimmune diabetes (57). Similarly, the islet BM of engrafted allogeneic islets as well as the excessive levels of perlecan$^+$ ECM that we observed within islet allograft sites would be expected to act as formidable barriers to intraislet MNC infiltration and intragraft migration during the allograft rejection response (33,47,57). The production of matrix-degrading enzymes such as heparanase by infiltrating host MNCs could circumvent this problem and potentially represent a novel drug target for anti-graft rejection therapy. Conversely, BM-deficient islets would be expected to be at a heightened risk of immune destruction.

In this study of islet BM matrix proteins, we revealed complete loss of the islet BM after islet isolation and a transient absence of a conventional islet BM and intraislet subvascular endothelial BM early after transplantation, which together highlight a period of islet vulnerability and increased risk of β-cell loss due to ECM detachment. We further identify critical roles for VEC migration and subendothelial BM remodeling in the reassembly of the islet BM in islet isografts and allografts and in the restoration of intraislet vasculature and β-cell–matrix attachment in islet isografts. We discovered that intraislet BMs fail to recover in islet allografts and postulate that prolonged matrix detachment from both peri- and intraislet BMs may negatively impact the survival of islet β-cells, supplementing MNC-mediated destruction of islet allografts in the absence of antirejection therapy. These findings strongly support the critical need for the islet BMs to be preserved during islet isolation. Potential benefits would include improvement in β-cell viability due to the maintenance of β-cell–matrix attachment, the possibility of more efficient revascularization of the engrafted islets, and the retention of a local BM barrier protection of allogeneic islets against cell invasion. Our studies identify the islet BM as a critical biomarker for islet integrity and predict that islet BM analysis after enzymatic isolation could be an effective measure for evaluating optimal enzyme preparations/combinations, particularly for clinical islet transplantation.

ACKNOWLEDGMENTS: We are grateful to Wendy Bonner for the preparation and staining of frozen tissue sections; to Sarah Popp and Dr Andrew Ziolkowski for assistance in flow cytometry studies; and to Debra Brown, Lora Jensen, and Peter Hamilton for technical assistance and animal care. This work was supported by a National Health and Medical Research Council of Australia (NH&MRC)/JDRF Special Program Grant in Type 1 Diabetes (#418138), the Diabetes Australia Research Trust Apex Award 2010, a NHMRC Program Grant (#455395), and a research grant from the Roche Organ Transplantation Research Foundation (ROTRF)/JDRF (#477554991). The authors declare no conflict of interest.

REFERENCES

1. Antonioli, B.; Fermo, I.; Cainarca, S.; Marzorati, S.; Nano, R.; Baldissera, M.; Bachi, A.; Paroni, R.; Ricordi, C.; Bertuzzi, F. Characterization of collagenase blend enzymes for human islet transplantation. Transplantation 84:1568–1575; 2007.
2. Balamurugan, A. N.; Loganathan, G.; Bellin, M. D.; Wilhelm, J. J.; Harmon, J.; Anazawa, T.; Soltani, S. M.; Radosevich, D. M.; Yuasa, T.; Tiwari, M.; Papas, K. K.; McCarthy, R.; Sutherland, D. E. R.; Hering, B. J. A new enzyme mixture to increase the yield and transplant rate of autologous and allogeneic human islet products. Transplantation 93:693–702; 2012.
3. Berman, J.; Stoner, G.; Dawe, C.; Rice, J.; Kingsbury, E. Histochemical demonstration of collagen fibers in ascorbic-acid-fed cell cultures. In Vitro 14:675–685; 1978.
4. Bonner-Weir, S.; Orci, L. New perspectives on the microvasculature of the islets of Langerhans in the rat. Diabetes 31:883–889; 1982.
5. Brissova, M.; Fowler, M.; Wiebe, P.; Shostak, A.; Shiota, M.; Radhika, A.; Lin, P. C.; Gannon, M.; Powers, A. C. Intraislet endothelial cells contribute to revascularization

of transplanted pancreatic islets. Diabetes 53:1318–1325; 2004.
6. Brissova, M.; Powers, A. C. Revascularization of transplanted islets: Can it be improved? Diabetes 57:2269–2271; 2008.
7. Brissova, M.; Shostak, A.; Shiota, M.; Wiebe, P. O.; Poffenberger, G.; Kantz, J.; Chen, Z.; Carr, C.; Jerome, W. G.; Chen, J.; Baldwin, H. S.; Nicholson, W.; Bader, D. M.; Jetton, T.; Gannon, M.; Powers, A. C. Pancreatic islet production of vascular endothelial growth factor-A is essential for islet vascularization, revascularization, and function. Diabetes 55:2974–2985; 2006.
8. Dziadek, M.; Paulsson, M.; Timpl, R. Identification and interaction repertoire of large forms of the basement membrane protein nidogen. EMBO J. 4:2513–2518; 1985.
9. Gazda, L. S.; Charlton, B.; Lafferty, K. J. Diabetes results from a late change in the autoimmune response of NOD mice. J. Autoimmun. 10:261–270; 1997.
10. Gibly, R. F.; Graham, J. G.; Luo, X.; Lowe, Jr., W. L.; Hering, B. J.; Shea, L. D. Advancing islet transplantation: From engraftment to the immune response. Diabetologia 54:2494–2505; 2011.
11. Gray, D. W. R.; Leow, C. K. Non-automated methods for islet isolation. In: Ricordi, C., ed. Pancreatic islet cell transplantation. Austin, TX: R. G. Landes; 1992:89–98.
12. Grossman, J. Molecular mechanisms of "detachment-induced apoptosis—Anoikis". Apoptosis 7:247–260; 2002.
13. Hammar, E.; Parnaud, G.; Bosco, D.; Perriraz, N.; Maedler, K.; Donath, M.; Rouiller, D. G.; Halban, P. A. Extracellular matrix protects pancreatic β-cells against apoptosis: Role of short- and long-term signaling pathways. Diabetes 53:2034–2041; 2004.
14. Hering, B. J.; Kandaswamy, R.; Harmon, J. V.; Ansite, J. D.; Clemmings, S. M.; Sakai, T.; Paraskevas, S.; Eckman, P. M.; Sageshima, J.; Nakano, M.; Sawada, T.; Matsumoto, I.; Zhang, H. J.; Sutherland, D. E.; Bluestone, J. A. Transplantation of cultured islets from two-layer preserved pancreases in type 1 diabetes with anti-CD3 antibody. Am. J. Transplant. 4:390–401; 2004.
15. Ichii, H.; Ricordi, C. Current status of islet cell transplantation. J. Hepatobiliary Pancreat. Surg. 16:101–112; 2009.
16. Iglesias I.; Valiente L.; Shiang K. D.; Ichii, H.; Kandeel, F.; Al-Abdullah, I. H. The effects of digestion enzymes on islet viability and cellular composition. Cell Transplant. 21:649–655; 2012.
17. Irving-Rodgers, H. F.; Ziolkowski, A. F.; Parish, C. R.; Sado, Y.; Ninomiya, Y.; Simeonovic, C. J.; Rodgers, R. J. Molecular composition of the peri-islet basement membrane in NOD mice: A barrier against destructive insulitis. Diabetologia 51:1680–1688; 2008.
18. Jansson, L.; Carlsson, P.-O. Graft vascular function after transplantation of pancreatic islets. Diabetologia 45:749–763; 2002.
19. Johansson, M.; Olerud, J.; Jansson, L.; Carlsson, P.-O. Prolactin treatment improves engraftment and function of transplanted pancreatic islets. Endocrinology 150:1646–1653; 2009.
20. Johansson, U.; Rasmusson, I.; Niclou, S. P.; Forslund, N.; Gustavsson, L.; Nilsson, B.; Korsgren, O.; Magnusson, P. U. Formation of composite endothelial cell-mesenchymal stem cell islets: A novel approach to promote islet revascularization. Diabetes 57:2393–2401; 2008.
21. Kilkenny, D. M.; Rocheleau, J. V. Fibroblast growth factor receptor-1 signaling in pancreatic islet β-cells is modulated by the extracellular matrix. Mol. Endocrinol. 22:196–205; 2008.
22. Konstantinova, I.; Lemmert, E. Microvascular development: Learning from pancreatic islets. BioEssays 26(10): 1069–1075; 2004.
23. Kragl, M.; Lammert, E. Basement membrane in pancreatic islet function. Adv. Exp. Med. Biol. 654:217–234; 2010.
24. Modlich, U.; Kaup, F. J.; Augustin, H. G. Cyclic angiogenesis and blood vessel regression in the ovary: Blood vessel regression during luteolysis involves endothelial cell detachment and vessel occlusion. Lab. Invest. 74:771–780; 1996.
25. Morini, S.; Brown, M. L.; Cicalese, L.; Elias, G.; Carotti, S.; Gaudio, E.; Rastellini, C. Revascularization and remodeling of pancreatic islets grafted under the kidney capsule. J. Anat. 210:565–577; 2007.
26. Neubauer, K.; Lindhorst, A.; Tron, K.; Ramadori, G.; Saile, B. Decrease of PECAM-1-gene-expression induced by proinflammatory cytokines IFN-γ and IFN-α is reversed by TGF-β in sinusoidal endothelial cells and hepatic mononuclear phagocytes. BMC Physiol. 8(9); 2008. doi: 10.1186/1472-6793-8-9
27. Nikolova, G.; Jabs, N.; Konstantinova, I.; Domogatskaya, A.; Tryggvason, K.; Sorokin, L.; Fassler, R.; Gu, G.; Gerber, H. P.; Ferrara, N.; Melton, D. A.; Lammert, E. The vascular basement membrane: A niche for insulin gene expression and β cell proliferation. Dev. Cell 10:397–405; 2006.
28. Nikolova, G.; Strilic, B.; Lammert, E. The vascular niche and its basement membrane. Trends Cell Biol. 17:19–25; 2007.
29. Nyqvist, D.; Kohler, M.; Wahlstedt, H.; Berggren, P.-O. Donor islet endothelial cells participate in formation of functional vessels within pancreatic islet grafts. Diabetes 54:2287–2293; 2005.
30. O'Gorman D.; Kin T.; Imes, S.; Pawlick, R.; Senior, P.; Shapiro, A. M. J. Comparison of human islet isolation outcomes using a new mammalian tissue-free enzyme versus collagenase NB-1. Transplantation 90:255–259; 2010.
31. Olsson, R.; Carlsson, P.-O. The pancreatic islet endothelial cell: Emerging roles in islet function and disease. Int. J. Biochem. Cell Biol. 38:492–497; 2006.
32. Papaccio, G.; Pisanti, F. A.; Montefiano, R. D.; Graziano, A.; Latronico, M. V. G. Th1 and Th2 cytokines exert regulatory effects upon islet microvascular areas in the NOD mouse. J. Cell. Biochem. 86:651–664; 2002.
33. Parish, C. R. The role of heparan sulphate in inflammation. Nat. Rev. Immunol. 6:633–643; 2006.
34. Parnaud, G.; Hammar, E.; Rouiller, D. G.; Armanet, M.; Halban, P. A.; Bosco, D. Blockade of β1 integrin-laminin-5 interaction affects spreading and insulin secretion of rat β-cells attached on extracellular matrix. Diabetes 55:1413–1420; 2006.
35. Paulsson, M. Basement membrane proteins: Structure, assembly, and cellular interactions. Crit. Rev. Biochem. Mol. Biol. 27:93–127; 1992.
36. Persson-Sjogren, S.; Forsgren, S.; Taljedal, I. B. Peptides and other neuronal markers in transplanted pancreatic islets. Peptides 21:741–752; 2000.
37. Pinkse, G. G. M.; Bouwman, W. P.; Jiawan-Lalai, R.; Terpstra, O. T.; Bruijn, J. A.; de Heer, E. Integrin signaling via RGD peptides and anti-β1 antibodies confers resistance to apoptosis in islets of Langerhans. Diabetes 55:312–317; 2006.
38. Pober, J. S.; Cotran, R. S. The role of endothelial cells in inflammation. Transplantation 50:537–544; 1990.
39. Puchtler, H.; Waldrop, F. W. Silver impregnation methods for reticulum fibers and reticulin: A re-investigation of their

origins and specificity. Histochemistry 57 (3):177–187; 1978.
40. Ricordi, C.; Alejandro, R.; Rilo, H. H.; Carroll, P. B.; Tzakis, A. G.; Starzl, T. E.; Mintz, D. H. Long-term in vivo function of human mantled islets obtained by incomplete pancreatic dissociation and purification. Transplant. Proc. 27:3382; 1995.
41. Rosenberg, L.; Wang, R.; Paraskevas, S.; Maysinger, D. Structural and functional changes resulting from islet isolation lead to islet cell death. Surgery 126:393–398; 1999.
42. Salvay, D. M.; Rives, C. B.; Zhang, X.; Chen, F.; Kaufman, D. B.; Lowe, Jr., W. L.; Shea, L. D. Extracellular matrix protein coated scaffolds promote the reversal of diabetes after extrahepatic islet transplantation. Transplantation 85:1456–1464; 2008.
43. Shapiro, A. M. J. State of the art of clinical islet transplantation and novel protocols of immunosuppression. Curr. Diab. Rep. 11:345–354; 2011.
44. Shapiro, A. M. J.; Lakey, J. R.; Ryan, E. A.; Korbutt, G. S.; Toth, E.; Warnock, G. L.; Kneteman, N. M.; Rajotte, R. V. Islet transplantation in seven patients with type 1 diabetes mellitus using a glucocorticoid-free immunosuppressive regimen. N. Engl. J. Med. 343:230–238; 2000.
45. Simeonovic, C. J.; Brown, D. J.; Townsend, M. J.; Wilson, J. D. Differences in the contribution of CD4+T cells to proislet and islet allograft rejection correlate with constitutive class II MHC alloantigen expression. Cell Transplant. 5:525–541; 1996.
46. Simeonovic, C. J.; Zarb, J. C.; Gazda, L. S.; Lafferty, K. J.; Wilson, J. D. Pancreatic islet and proislet transplantation in the mouse model. In: Timmermann, W.; Ulrichs, K.; Thiede D. A., eds. Microsurgical models in rats and mice for transplantation research. Berlin: Springer-Verlag; 1998:167–177.
47. Sorokin, L. The impact of the extracellular matrix on inflammation. Nat. Rev. Immunol. 10:712–723; 2010.
48. Spring, H.; Schuler, T.; Arnold, B.; Hammerling, G. J.; Ganss, R. Chemokines direct endothelial progenitors into tumor neovessels. Proc. Natl. Acad Sci. USA 102:18111–18116; 2005.
49. Stewart, R. J.; Kashour, T. S.; Marsden, P. A. Vascular endothelial platelet endothelial cell adhesion molecule-1 (PECAM-1) expression is decreased by TNF-α and IFN-γ. Evidence for cytokine-induced destabilization of messenger ribonucleic acid transcripts in bovine endothelial cells. J. Immunol. 156:1221–1228; 1996.
50. Thomas, F.; Wu, J.; Contreras, J. L.; Smyth, C.; Bilbao, G.; He, J.; Thomas, J. A tripartite anoikis-like mechanism causes early isolated islet apoptosis. Surgery 130:333–338; 2001.
51. Thomas, F. T.; Contreras, J. L.; Bilbao, G.; Ricordi, C.; Curiel, D.; Thomas, J. M. Anoikis, extracellular matrix, and apoptosis factors in isolated cell transplantation. Surgery 126:299–304; 1999.
52. Vajkoczy, P.; Olofsson, A. M.; Lehr, H. A.; Leiderer, R.; Hammersen, F.; Arfors, K. E.; Menger, M. D. Histogenesis and ultrastructure of pancreatic islet graft microvasculature. Am. J. Pathol. 146:1397–1405; 1995.
53. Virtanen, I.; Banerjee, M.; Palgi, J.; Korsgren, O.; Lukinius, A.; Thornell, L. E.; Kikkawa, Y.; Sekiguchi, K.; Hukkanen, M.; Konttinen, Y. T.; Otonkoski, T. Blood vessels of human islets of Langerhans are surrounded by a double basement membrane. Diabetologia 51:1181–1191; 2008.
54. Wang, R. N.; Paraskevas, S.; Rosenberg, L. Characterization of integrin expression in islets isolated from hamster, canine, porcine, and human pancreas. J. Histochem. Cytochem. 47:499–506; 1999.
55. Wang, R. N.; Rosenberg, L. Maintenance of beta cell function and survival following islet isolation requires re-establishment of the islet-matrix relationship. J. Endocrinol. 163:181–190; 1999.
56. Weber, L. M.; Anseth, K. S. Hydrogel encapsulation environments functionalized with extracellular matrix interactions increase islet insulin secretion. Matrix Biol. 27:667–673; 2008.
57. Ziolkowski, A. F.; Popp, S. K.; Freeman, C.; Parish, C. R.; Simeonovic, C. J. Heparan sulfate and heparanase play key roles in mouse β cell survival and autoimmune diabetes. J. Clin. Invest. 122:132–141; 2012.